# EFFICIENT INCOMPLETE MULTI-VIEW CLUSTERING VIA FLEXIBLE ANCHOR LEARNING

**Anonymous authors**
Paper under double-blind review

## ABSTRACT

Multi-view clustering aims to improve the final performance by taking advantages of complementary and consistent information of all views. In real world, data samples with partially available information are common and the issue regarding the clustering for incomplete multi-view data is inevitably raised. To deal with the partial data with large scales, some fast clustering approaches for incomplete multi-view data have been presented. Despite the significant success, few of these methods pay attention to learning anchors with high quality in a unified framework for incomplete multi-view clustering, while ensuring the scalability for large-scale incomplete datasets. In addition, most existing approaches based on incomplete multi-view clustering ignore to build the relation between anchor graph and similarity matrix in symmetric nonnegative matrix factorization and then directly conduct graph partition based on the anchor graph to reduce the space and time consumption. In this paper, we propose a novel fast incomplete multi-view clustering method for the data with large scales, termed Efficient Incomplete Multi-view clustering via flexible anchor Learning (EIML), where graph construction, anchor learning and graph partition are simultaneously integrated into a unified framework for efficient incomplete multi-view clustering. To be specific, we learn a shared anchor graph to guarantee the consistency among multiple views and employ a adaptive weight coefficient to balance the impact for each view. The relation between anchor graph and similarity matrix in symmetric nonnegative matrix factorization can also be built, i.e., each entry in the anchor graph can characterize the similarity between the anchor and original data sample. We then adopt an alternative algorithm for solving the formulated problem. Experiments conducted on different datasets confirm the superiority of EIML compared with other clustering methods for incomplete multi-view data. paragraph.

## 1 INTRODUCTION

In real application, data are usually represented with different features from multiple views. This kind of data is usually named multi-view data and integrating the various information for clustering has shown to be a critical task in the unsupervised learning field. By investigating the complementary and diverse information among different views, a large number of clustering methods for multi-view data have been given Zhang et al. (2021a); Kumar et al. (2011); Qin et al. (2022); Chen et al. (2022); Zhao et al. (2023); Wang et al. (2023); Yu et al. (2023); Jia et al. (2023) in recent years. For instance, Kumar et al. Kumar et al. (2011) guaranteed that different representations are able to agree with each other by co-regularizing the clustering hypotheses. Ye et al. Ye et al. (2016) maximized the sum of weighted similarities among multiple clusterings to study the underlying clustering. Nie et al. Nie et al. (2017) simultaneously learned the local structure as well as performed semi-supervised classification or clustering. Luo et al. Luo et al. (2018) studied specificity and consistency in the representations from different views. Chen et al. Chen et al. (2020) jointly explored the affinity matrix as well as the low-rank representation tensor. Zhou et al. Zhou et al. (2020) utilized the predefined kernels to learn a consistent representation or a shared kernel and then achieved the unified clustering results. The vital part of clustering for multi-view data is to study the consistency of different views by learning a unified representation. Most existing multi-view clustering works make the assumption that data samples from different views are available Zhao et al. (2017); Zhang et al. (2021b).

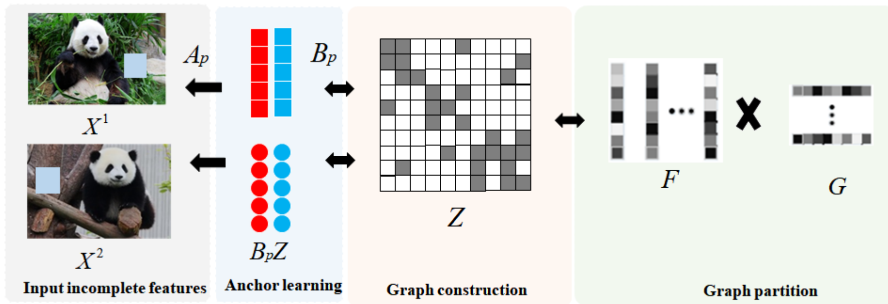


Figure 1: Framework of EIML. It jointly models graph construction, anchor learning and graph partition in a unified framework for efficient incomplete multi-view clustering. To be specific, $X^1$ and $X^2$ are incomplete multi-view datasets as input, $B_p$ denotes the projection as the anchor guidance, $A_p$ is the indicator representation for the missing data, $Z$ refers to the shared anchor graph, $G$ and $F$ denote the centroid matrix and cluster assignment, respectively.

However, data samples in most applications often lack the information for some views Xu et al. (2023; 2019); Qin et al. (2023); Lv et al. (2022). Then the approaches based on integrity have difficulty in dealing with incomplete data from multiple views. In order to handle such problem, several methods of incomplete multi-view clustering have been presented Zhang et al. (2020). We can conclude these methods into three strategies including graph construction, matrix factorization and deep learning. The methods based on graph construction aim to produce a similarity matrix shared by different views. For instance, Liu et al. Liu et al. (2017) simultaneously learned a representation and filled in the blank value. The methods based on matrix factorization make full use of $L_1$ constraint and nonnegative matrix factorization to learn a consensus representation Li et al. (2014). Shao et al. Shao et al. (2015) integrated weighted matrix factorization and $L_{2,1}$ regularization to obtain better clustering performance. The methods based on deep learning use a deep neural network to recover the missing data and the feature representation. As a representative, Lin et al. Lin et al. (2021) employed contrastive learning for integrating data recovery and feature learning. However, most existing methods easily suffer from the high computation and space cost, which inevitably restricts their availability on the datasets with large scales.

To cope with the above issue, many methods for the data with large scales have been proposed. Wang et al. Wang et al. (2011) built a constrained factor matrix for exploring the cluster structure. Kang et al. Kang et al. (2020) employed $K$-means to obtain the anchors and then collocated them for a unified representation. Li et al. Li et al. (2022) adopted the consistent learned anchors for handling the clustering problems of incomplete multi-view data. Nie et al. Nie et al. (2020) simultaneously performed clustering on column and row of the original dataset. Wang et al. Wang et al. (2022b) used the guidance of consensus anchors to study the anchor graph shared by different views. Sun et al. Sun et al. (2021) exploited the underlying distribution of the data to construct the anchor graph. Among these existing methods, the approaches based on anchor have achieved attention due to the scalability and efficiency. This kind of methods usually employs the original data and the generated anchors to build the corresponding anchor graph, resulting in more satisfied clustering performance. Despite great success, the above methods neglect learning high-quality anchors in a unified framework for incomplete multi-view clustering, while ensuring the scalability for incomplete datasets with large scales. In addition, few of the existing approaches based on incomplete multi-view clustering pay attention to building the relation between anchor graph and similarity matrix in symmetric nonnegative matrix factorization and then directly performing graph partition based on the anchor graph for reducing the space and computation consumption.

In this paper, we propose a novel fast incomplete multi-view clustering method for the data with large scales, termed Efficient Incomplete Multi-view clustering via flexible anchor Learning (EIML), where graph construction, anchor learning and graph partition are simultaneously considered in a unified framework for efficient incomplete multi-view clustering as Fig. 1. These three parts can boost each other, which promotes the quality of the clustering and improves the efficiency for large scale datasets. To be specific, we learn a shared anchor graph to guarantee the consistency among multiple views and adopt a adaptive weight coefficient to balance the impact for each view. The relation between anchor graph and similarity matrix in symmetric nonnegative matrix factorization can also be built, i.e., each entry in the anchor graph can describe the similarity between the anchor and original data sample. In particular, we constrain the factor matrix to be a cluster indicator representation by introducing the orthogonal constraint on the actual bases. Furthermore, we adopt the alternative algorithm for solving the optimization problem.

As a summary, the proposed EIML has the main contributions in the following:

- We give a new insight to the community of incomplete multi-view clustering for large scale datasets, i.e., graph construction, anchor learning and graph partition in efficient incomplete multi-view clustering can boost each other, which are able to be integrated into a problem. The combination of these three issues is the focus in our work. While most existing work treat graph construction, anchor learning and graph partition as separated problems in incomplete multi-view clustering for the datasets with large scales.
- We propose a novel fast incomplete multi-view clustering method for large scale data termed as EIML, where graph construction, anchor learning and graph partition are simultaneously considered in a unified framework for efficient incomplete multi-view clustering. The relation between anchor graph and similarity matrix in symmetric nonnegative matrix factorization is also built, i.e., each entry in the anchor graph is able to characterize the similarity between the anchor and original data sample.
- Based on the relation between anchor graph and similarity matrix, we constrain the factor matrix with rigorous interpretation to be cluster indicator representation by introducing the orthogonal constraint on the actual bases and use the alternative algorithm for solving the formulated problem. Extensive experiments are performed on different datasets to demonstrate the superiority of EIML in terms of effectiveness and efficiency.

## 2 Efficient Incomplete Multi-view Clustering via Flexible Anchor Learning

This section begins with introducing the motivation and formulation of the proposed EIML, then moves on to the detailed optimization process for EIML. We lastly conduct the analysis about the computation complexity to demonstrate the efficiency of EIML.

**Motivation:** For large-scale incomplete data clustering, reducing the redundancy of the data is the key to increase efficiency. Some existing works denote each data sample with a linear combination of the others and the global relation can be well exploited in this manner. However, the relatively high storage and computation time produced in this way inevitably limit the scalability of incomplete multi-view clustering for large-scale dataset. Actually, relatively less data samples are enough to reconstruct the latent space. Therefore, selecting some data samples from the original dataset as anchors or landmarks for reconstructing the relation structure is commonly used in the existing works.

Nevertheless, some existing incomplete multi-view clustering approaches usually conduct strategies based on heuristic sampling, where the anchor selection and graph construction are separated. Then the graph is constructed after selecting the anchors for different views. In this manner, the complementary information among different views is not able to be well explored and further algorithm is needed to obtain a shared graph. Afterwards, the clustering algorithm (spectral clustering) is usually needed to achieve the final clustering results. This multiple-stage process significantly affects the quality of the anchors. Besides, few of the existing methods pay attention to building the relation between anchor and similarity matrix in symmetric nonnegative matrix factorization. As is known, each entry of a similarity matrix can describe the similarity between data samples in the dataset. Performing symmetric nonnegative matrix factorization for the similarity matrix can directly lead to the final partition. Then building the relation between anchor and similarity matrix can take advantages of directly obtaining the final clustering results in incomplete multi-view clustering. How to learn anchors with high quality in a unified framework and build the relation between anchor graph and similarity matrix in symmetric nonnegative matrix factorization to ensure the scalability on large-scale dataset for incomplete multi-view clustering remains a considerably challenging issue.

**Formulation:** Different from most existing works for incomplete multi-view clustering, we learn anchors instead of selecting them based on the available data samples in the dataset. The proposed EIML integrates graph construction, anchor learning and graph partition into a unified framework for efficient incomplete multi-view clustering. Then the discriminative anchors are automatically learned and the final partition can be achieved in this manner. Based on the assumption that multiple views are sampled from a latent space, the anchors from multiple views are expected to be consistent in this space. Given multi-view dataset $\{X_p\}_{p=1}^v$, we construct the projection $B_p \in R^{d_p \times m}$ as the consensus anchor guidance to integrate complementary information from different views into the shared anchor graph $Z \in R^{m \times n}$, where $d_p$ and $m$ are the dimension of the data and the total number of anchors for the $p$-th view, respectively. The indicator representation $A_p \in \{0,1\}^{n \times n_p}$ is adopted to mark the unavailable data samples. The above process can be formulated as follows:

$$\min_{\alpha, Z, \{B_p\}_{p=1}^v} \sum_{p=1}^{v} \alpha_p^2 \|X_p A_p - B_p Z A_p\|_F^2, \;\; s.t. \; \alpha^T \mathbf{1} = 1, \; B_p^T B_p = I, \; Z \geq 0, \; Z^T \mathbf{1} = 1, \tag{1}$$

where $\alpha_p^2$ is the coefficient of each view. It can be learned based on the contribution to the shared anchor graph. $X_p A_p$ denotes the available data samples for the $p$-th view. Since the space complexity of anchor graph $Z$ is $O(m \times n)$, we can relate $Z$ with similarity matrix in symmetric nonnegative matrix factorization for directly obtaining the final partition. As is known, symmetric nonnegative similarity matrix with the space complexity $O(n \times n)$ can be adopted to achieve the final clustering results based on factorization. Each entry in the anchor graph $Z$ describes the similarity between data sample and anchor. Since the symmetric constraint on $Z \in R^{m \times n}$ are not guaranteed in factorization with $m \ll n$, we remove such constraint on anchor graph $Z$ and this is the main difference between anchor graph and similarity matrix in symmetric nonnegative matrix factorization. We then introduce the centroid matrix $G \in R^{m \times k}$ and the cluster assignment $F \in R^{k \times n}$ with $k$ being the total number of clusters in the dataset as follows:

$$\min_{G,F} \|Z - GF\|_F^2, \;\; s.t. \; G^T G = I, \; F_{ij} \in \{0,1\}, \;\; \forall j = 1, \; 2, \; \cdots, \; n, \; \sum_{i=1}^{k} F_{ij} = 1, \tag{2}$$

where $F_{ij} = 0$ if the $j$-th data sample is not belonged to the $i$-th cluster and 1 otherwise. Note that imposing the orthogonal constraint on the actual bases can guide learning the factor matrix with rigorous clustering interpretation. To combine the partition information into the unified model, we formulate the total objective function as:

$$\begin{aligned} &\min_{G,F,\alpha,Z,\{B_p\}_{p=1}^v} \sum_{p=1}^{v} \alpha_p^2 \|X_p A_p - B_p Z A_p\|_F^2 + \lambda \|Z - GF\|_F^2, \; s.t. \; G^T G = I, \\ &\sum_{i=1}^{k} F_{ij} = 1, \; F_{ij} \in \{0,1\}, \; \forall j = 1, \; 2, \; \cdots, \; n, \;\; \alpha^T \mathbf{1} = 1, \; B_p^T B_p = I, \; Z \geq 0, \; Z^T \mathbf{1} = 1, \end{aligned} \tag{3}$$

where $\lambda > 0$ denotes the parameter for balancing different terms. Then graph construction, anchor learning and graph partition are jointly integrated into a unified framework for incomplete multi-view clustering in this manner, where these three parts can boost each other to achieve effective and efficient clustering results for incomplete large-scale multi-view dataset.

**Optimization:** We then design an alternating algorithm for optimizing each variable in Eq. (3) by fixing the others.

**(1) Optimize $\{B_p\}_{p=1}^v$:** With other variables being fixed, the objective function for $\{B_p\}_{p=1}^v$ can be rewritten as

$$\min_{\{B_p\}_{p=1}^v} \sum_{p=1}^{v} \alpha_p^2 \|X_p A_p - B_p Z A_p\|_F^2, \;\; s.t. \; B_p^T B_p = I. \tag{4}$$

We can remove the irrelevant items and transform Eq. (4) into the form as follows:

$$\max_{B_p} Tr(B_p \Lambda_p), \;\; s.t. \; B_p^T B_p = I, \tag{5}$$

where $\Lambda_p = (X_p \otimes H_p) Z^T$, $\otimes$ denotes the Hadamard product, $H_p = 1_{d_p} a_p$, $a_p = [a_{p,1}, \cdots, a_{p,n}]^T$ and $a_{p,j} = \sum_{l=1}^{n_p} A_{p,l,j}$. After conducting the singular value decomposition on $\Lambda_p$, the optimal solution of $B_p$ can be derived as $\Xi_m \Psi_m^T$, where $\Xi_m$ and $\Psi_m$ represent the matrices with the first $m$ singular vectors of $\Lambda_p$ in the left and right, respectively.

**(2) Optimize $Z$** : With others being fixed, the objective for $Z$ turns to solve the problem as:

$$\min_{Z} \sum_{p=1}^{v} \alpha_p^2 \|X_p A_p - B_p Z A_p\|_F^2 + \lambda \|Z - GF\|_F^2, \;\; s.t.\; Z \geq 0,\; Z^T \mathbf{1} = 1. \tag{6}$$

We then remove the irrelevant items and rewrite Eq. (6) as follows:

$$\min_{Z} \sum_{p=1}^{v} \alpha_p^2 Tr(Z^T Z(Q_p + \frac{\lambda}{\alpha_p^2} I) - 2X_p^T B_p Z Q_p - 2\frac{\lambda}{\alpha_p^2} Z^T GF),\; s.t.\; Z \geq 0,\; Z^T \mathbf{1} = 1, \tag{7}$$

where $Q_p = A_p A_p^T$. Since $z_i$ can be denoted as a vector with $z_{j,i}$ being the $j$-th entry, we can solve Eq. (7) by column as follows:

$$\min_{z_i} \|z_i - y_i\|_F^2, \;\; s.t.\; z_i \geq 0,\; z_i^T \mathbf{1} = 1, \tag{8}$$

where $y_i^T = \sum_{p=1}^{v} \alpha_p^2 H_{p,i,j} X_{p,:,i}^T B_p / \lambda + \sum_{p=1}^{v} \alpha_p^2 H_{p,i,j}$. We then rewrite the Lagrangian function of Eq. (8) as:

$$L(z_i, \sigma_i, \gamma_i) = \|z_i - y_i\|_F^2 - \gamma_i^T z_i - \sigma_i (z_i^T 1 - 1), \tag{9}$$

where $\sigma_i$ and $\gamma_i$ correspond to Lagrangian multipliers. With KKT conditions, we have the equation:

$$\begin{cases} z_i - y_i - \sigma_i 1 - \gamma_i = 0 \\ \gamma_i \otimes z_i = 0. \end{cases} \tag{10}$$

Combining the constraint $z_i^T \mathbf{1} = 1$, we can obtain the equation as follows:

$$z_i = \max(y_i + \sigma_i 1, 0), \;\; \sigma_i = \frac{1 + y_i^T 1}{m}. \tag{11}$$

**(3) Optimize $G$**: With other variables being fixed, the objective function for $G$ is transformed into the problem as follows:

$$\min_{G} \lambda \|Z - GF\|_F^2, \;\; s.t.\; G^T G = I. \tag{12}$$

The optimization for $G$ can be written as

$$\max_{G} Tr(G^T J), \;\; s.t.\; G^T G = I, \tag{13}$$

where $J = ZF^T$. Then the optimal solution for $G$ is $U_J V_J^T$ with $J = U_J \Sigma_J V_J^T$ based on singular value decomposition (SVD).

**(4) Optimize$F$**: With other variables being fixed, the objective function for $F$ can be formulated as the minimization problem as:

$$\min_{F} \lambda \|Z - GF\|_F^2, \;\; s.t.\; F_{ij} \in \{0, 1\},\; \forall j = 1,\; 2,\; \cdots,\; n, \sum_{i=1}^{k} F_{ij} = 1, \tag{14}$$

We then have the minimization problem as

$$\min_{F_{:,j}} \lambda \|Z_{:,j} - GF_{:,j}\|^2, \;\; s.t.\; F_{:,j} \in \{0, 1\}^k,\; \|F_{:,j}\|_1 = 1. \tag{15}$$

Then the optimal row can be achieved by

$$i^* = \arg\min_{i} \|S_{:,j} - G_{:,i}\|^2. \tag{16}$$

According to Eq. (16), we can find that the optimal cluster assignment is achieved by the cluster centroid and the object.

**(5) Optimize $\alpha_p^v$**: With other variables being fixed, the objective function for $\alpha_p^v$ is:

$$\min_{\alpha} \sum_{p=1}^{v} \alpha_p^2 \kappa_p, \;\; s.t.\; \alpha^T \mathbf{1} = 1,\; \alpha \geq 0, \tag{17}$$

where $\kappa_p = \|X_p A_p - B_p Z A_p\|_F^2$. We can obtain the optimal $\alpha$ based on Cauchy-Schwarz inequality as:

$$\alpha = \frac{\delta}{\sum_{p=1}^{v} \delta_p}, \tag{18}$$

where $\delta = [\delta_1,\; ...,\; \delta_v]$ with $\delta_p = 1/\kappa_p$.

### 2.1 Complexity Analysis

The computation burden of EIML consists of the optimization cost of each variable. To be specific, the time complexity for optimizing $B_p$ is $O(m^2d + mnd)$ at each iteration. Optimizing the weight $\alpha$ of each view costs $O(mnd)$. The time cost to learn the shared anchor graph $Z$ is $O(mnd)$. For optimizing $F$, the time cost is $O(mnk)$. The time cost to update $G$ is $O(mk^2)$. Then the total time complexity of the proposed EIML is $O((m^2d+mnd+mnk+mk^2)t)$, where $t$ denotes the number of iterations for these parts. Due to $n \gg m$ and $n \gg k$, the computation cost of EIML is nearly linear to the size of the dataset $O(n)$.

---

**Algorithm 1:** Algorithm of EIML

---

**Input:** Incomplete multi-view dataset $\{X_p\}_{p=1}^{v}$, the total number of clusters $k$ and the missing indicator $\{H_p\}_{p=1}^{v}$.
**Output:** The final cluster assignment $F$.
**Initialize:** Initialize $Z$, $\{B_p\}_{p=1}^{v}$ and $\{\alpha_p\}_{p=1}^{v}$.
**repeat**
    Update $Z$ by solving the problem in Eq. (6);
    Update $\{B_p\}_{p=1}^{v}$ by solving the problem in Eq. (4);
    Update $G$ by solving the problem in Eq. (12);
    Update $F$ by solving the problem in Eq. (14);
    Update $\alpha$ by solving the problem in Eq. (17);
**until** *convergence*;

---

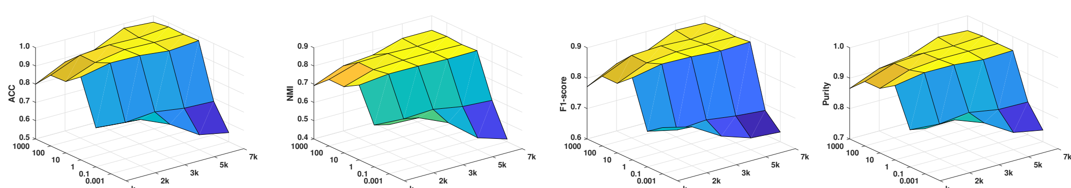

(a) ACC (b) NMI (c) F1-score (d) Purity

Figure 2: Parameter Study of $m$ and $\lambda$ on NGs in terms of four metrics.

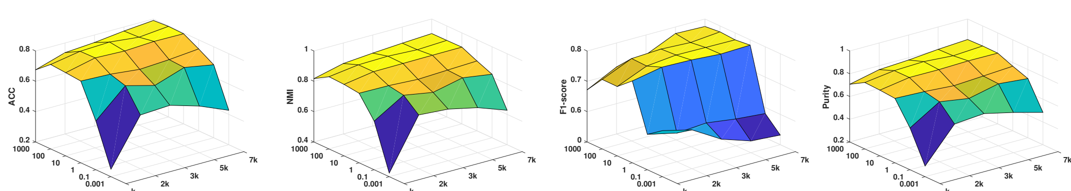

(a) ACC (b) NMI (c) F1-score (d) Purity

Figure 3: Parameter Study of $m$ and $\lambda$ on ORL in terms of four metrics.

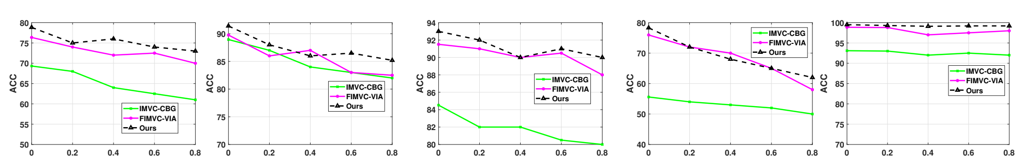


(a) ORL (b) NGs (c) WebKB (d) STL10 (e) Cifar100

Figure 4: Clustering Performance in terms of ACC on datasets with different missing ratios.

Table 1: Clustering Performance based on ACC (%) on datasets. “N/A ” denotes out of memory.

| Dataset | BSV | MIC | MKKM-IK | DAIMC | APMC | PIC | EEIMVC | $V^3$ | IMVC-CBG | FIMVC-VIA | Ours |
|---|---|---|---|---|---|---|---|---|---|---|---|
| ORL | 24.30±0.50 | 37.60±1.50 | 59.90±2.00 | 68.00±2.30 | 65.50±1.60 | 69.00±1.50 | 73.20±2.40 | 67.00±1.30 | 69.50±2.00 | 76.30±2.70 | 78.84±0.50 |
| NGs | 41.20±2.00 | 21.20±0.50 | 80.20±0.00 | 89.50±0.05 | 89.40±0.05 | 82.00±0.20 | 77.90±0.15 | 79.90±0.40 | 88.90±0.15 | 89.70±0.05 | 91.40±0.40 |
| WebKB | 57.00±2.20 | 63.80±0.50 | 68.00±0.00 | N/A | 85.30±0.05 | 71.60±0.00 | 61.80±3.40 | 75.20±0.50 | 84.50±0.50 | 91.50±0.50 | 93.00±0.26 |
| STL10 | 11.20±0.10 | N/A | 75.80±0.30 | 23.00±1.50 | 27.00±0.50 | 28.80±0.20 | 46.70±2.30 | 18.50±0.50 | 55.60±0.80 | 76.00±0.30 | 78.30±0.60 |
| MNIST | N/A | N/A | N/A | 97.60±0.50 | N/A | N/A | N/A | N/A | 98.20±0.05 | 98.75±0.30 | 98.90±0.00 |
| Cifar100 | N/A | N/A | N/A | 89.68±0.50 | N/A | N/A | N/A | N/A | 93.00±1.20 | 98.90±0.60 | 99.50±0.26 |

Table 2: Clustering Performance based on NMI (%) on datasets. “N/A ” denotes out of memory.

| Dataset | BSV | MIC | MKKM-IK | DAIMC | APMC | PIC | EEIMVC | $V^3$ | IMVC-CBG | FIMVC-VIA | Ours |
|---|---|---|---|---|---|---|---|---|---|---|---|
| ORL | 48.52±0.80 | 56.50±0.80 | 76.20±1.00 | 83.00±1.10 | 80.30±0.80 | 83.20±0.50 | 85.40±1.30 | 81.00±0.50 | 81.20±1.50 | 88.00±1.30 | 90.15±0.60 |
| NGs | 20.20±1.30 | 2.30±0.50 | 63.10±0.10 | 73.40±0.05 | 73.41±0.20 | 65.60±0.10 | 57.20±0.20 | 59.00±0.40 | 73.00±0.05 | 75.50±0.05 | 77.00±0.18 |
| WebKB | 1.85±0.80 | 3.30±0.50 | 4.00±0.10 | N/A | 47.90±0.20 | 1.70±0.00 | 3.50±0.50 | 23.60±1.00 | 37.20±0.15 | 48.90±0.20 | 51.20±0.50 |
| STL10 | 0.16±0.20 | N/A | 60.30±0.40 | 5.00±1.20 | 11.00±0.90 | 14.20±0.15 | 29.80±3.00 | 5.90±0.50 | 27.20±0.20 | 57.35±0.20 | 59.80±0.50 |
| MNIST | N/A | N/A | N/A | 93.90±0.50 | N/A | N/A | N/A | N/A | 94.90±0.10 | 96.20±0.30 | 97.30±0.10 |
| Cifar100 | N/A | N/A | N/A | 98.20±0.20 | N/A | N/A | N/A | N/A | 98.60±0.30 | 99.70±0.10 | 99.80±0.20 |

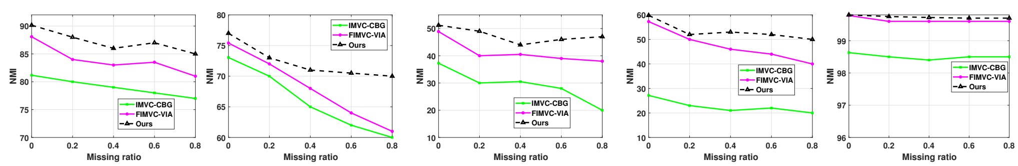

(a) ORL (b) NGs (c) WebKB (d) STL10 (e) Cifar100

Figure 5: Clustering Performance in terms of NMI on datasets with different missing ratios.

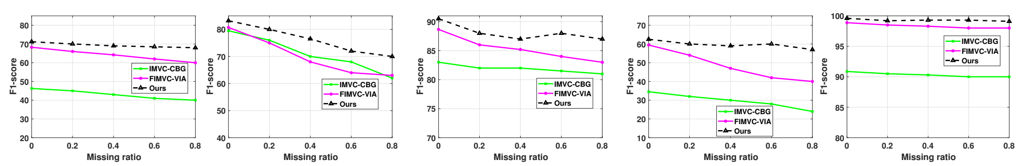

(a) ORL (b) NGs (c) WebKB (d) STL10 (e) Cifar100

Figure 6: Clustering Performance in terms of F1-score on datasets with different missing ratios.

## 3 Experiments

In this section, we perform experiments to validate the effectiveness and efficiency of EIML on several widely used multi-view datasets. Among these datasets, there are some large-scale datasets for better verifying the clustering performance and running time of EIML.

### 3.1 Datasets and Compared Methods

The experiments are conducted on several widely adopted datasets including news groups (NGs), WebKB, ORL, STL10, MNIST and Cifar100. **NGs** has total three preprocessings including partitioning around medoids, supervised mutual information and unsupervised mutual information. **WebKB** has two views. It is a dataset of web page including the content and citations collected from different universities’ websites. **ORL** has total 40 objects. It consists of frontal images in ten scenarios. Different facial details and lighting settings of an object produce differences among data samples. **STL10** has different types of transport and animal images. Features of images in this dataset are extracted based on three different ResNets as different views. **MNIST** contains total ten numbers from 0 to 9. It is a handwritten dataset provided by NIST. **Cifar100** has total three views and 5000 tiny images. The images of this dataset are tagged with 100 labels.

Table 3: Clustering Performance based on F1-score (%) on datasets. “N/A ” denotes out of memory.

| Dataset | BSV | MIC | MKKM-IK | DAIMC | APMC | PIC | EEIMVC | $V^3$ | IMVC-CBG | FIMVC-VIA | Ours |
|---|---|---|---|---|---|---|---|---|---|---|---|
| ORL | 9.00±0.50 | 17.50±1.00 | 46.30±2.30 | 56.80±2.60 | 50.50±2.40 | 57.70±1.30 | 63.50±2.90 | 55.00±1.50 | 46.30±3.00 | 68.20±3.00 | 71.20±0.50 |
| NGs | 32.30±1.00 | 32.80±0.20 | 68.70±0.00 | 80.30±0.05 | 80.40±0.60 | 72.80±0.20 | 64.00±0.20 | 65.60±0.40 | 79.50±0.05 | 80.80±0.00 | 83.20±0.70 |
| WebKB | 60.50±1.50 | 62.00±0.50 | 64.60±0.30 | N/A | 85.00±0.05 | 73.60±0.00 | 62.80±0.20 | 71.90±0.40 | 83.00±0.07 | 88.70±0.05 | 90.50±0.05 |
| STL10 | 11.70±0.05 | N/A | 57.80±0.30 | 13.20±1.80 | 18.60±1.20 | 21.40±0.10 | 29.90±2.00 | 17.05±0.50 | 34.60±0.07 | 59.90±0.00 | 62.50±0.50 |
| MNIST | N/A | N/A | N/A | 95.50±0.30 | N/A | N/A | N/A | N/A | 96.20±0.10 | 97.50±0.50 | 99.20±0.10 |
| Cifar100 | N/A | N/A | N/A | 90.50±0.50 | N/A | N/A | N/A | N/A | 91.90±0.50 | 99.00±0.50 | 99.60±0.20 |

Table 4: Clustering Performance based on Purity (%) on datasets. “N/A ” denotes out of memory.

| Dataset | BSV | MIC | MKKM-IK | DAIMC | APMC | PIC | EEIMVC | $V^3$ | IMVC-CBG | FIMVC-VIA | Ours |
|---|---|---|---|---|---|---|---|---|---|---|---|
| ORL | 26.90±0.90 | 40.50±1.50 | 63.00±2.00 | 71.90±1.60 | 69.30±1.20 | 72.30±1.00 | 76.00±2.10 | 70.20±1.00 | 69.30±1.80 | 79.10±2.00 | 82.50±0.29 |
| NGs | 43.10±1.50 | 21.50±0.50 | 79.60±0.05 | 89.50±0.05 | 89.42±0.05 | 82.40±0.20 | 77.80±0.10 | 79.80±0.40 | 88.70±0.05 | 90.00±0.06 | 93.12±0.05 |
| WebKB | 78.20±0.20 | 78.24±0.60 | 78.40±0.05 | N/A | 90.15±0.08 | 78.20±0.40 | 78.18±0.30 | 91.70±3.00 | 84.60±0.05 | 91.60±0.20 | 94.10±0.20 |
| STL10 | 11.30±0.05 | N/A | 75.80±0.30 | 23.20±1.80 | 27.60±1.20 | 29.30±0.15 | 46.90±2.00 | 18.60±0.50 | 55.60±0.08 | 76.00±0.20 | 78.90±0.55 |
| MNIST | N/A | N/A | N/A | 97.50±0.30 | N/A | N/A | N/A | N/A | 98.00±0.10 | 98.50±0.50 | 99.20±0.10 |
| Cifar100 | N/A | N/A | N/A | 92.50±0.50 | N/A | N/A | N/A | N/A | 94.90±0.50 | 99.00±0.50 | 99.55±0.20 |

We compare EIML with some representive incomplete multi-view clustering approaches in the following. **BSV** Ng et al. (2001) uses mean value filling to perform spectral clustering for each view and then gives the best single view result. **MIC** Shao et al. (2015) learns latent subspaces from different views and then performs optimization on a shared representation. **MKKM-IK** Ma et al. (2021) simultaneously imputes the missing part and performs kernel $K$-means algorithm. **DAIMIC** Hu & Chen (2018) deals with the problem of missing view by introducing a view-specific weight representation and then aligns the basis representations. **APMC** Guo & Ye (2019) uses the presented data samples from different views as anchors and achieves the final result by spectral clustering. **PIC** Wang et al. (2019) pads the similarity matrix by solving the problem of missing view. **EEIMVC** Liu et al. (2021) produces the base representations with low dimensions and then adopts a unified framework to simultaneously impute these representations and optimize a shared representation feature. $\boldsymbol{V^3}$**H** Fang et al. (2020) exploits the unique and consistent par among different incomplete views, which is motivated by genetics. **IMVC-CBG** Wang et al. (2022a) adopts a scalable anchor graph framework for the problem of incomplete multi-view clustering. **FIMVC-VIA** Liu et al. (2022) learns view-specific anchors and builds a consensus anchor graph shared by different views for incomplete multi-view clustering.

In the experiment, we use four metrics to evaluate the experimental results, which include accuracy (ACC), NMI, F1-score and Purity. We repeat each algorithm for total 20 times and then report the mean and standard deviation of the results. The parameters for the compared methods of incomplete multi-view clustering are set as their recommended ones. We run all experiments on AMD Ryzen 5 Six-Core Processor 3.60 GHz.

### 3.2 Parameter Selection

There are total two parameters appeared in EIML, including the trade-off parameter $\lambda$ and the number of anchors $m$. We then perform experiments on different datasets to study how these two parameters influence the final clustering performance. We set $\lambda$ and $m$ in the range of $[0.001, 0.1, 1, 10, 100, 1000]$ and $[k, 2k, 3k, 5k, 7k]$, respectively. Here, $k$ corresponds to the total number of clusters in dataset. According to Figs. 2-3, we find that better performance is achieved when $\lambda = 1$ under the same $m$ on different datasets. Besides, the clustering result of EIML is relatively stable over different parameter values on these datasets, which shows that EIML is generally robust to the trade-off parameter $\lambda$. It can also be observed that different number of anchors $m$ has relatively little influence on the clustering performance under the same $\lambda$ for these datasets.

### 3.3 Experimental Results

We list the detailed clustering results of EIML and the compared approaches on different datasets in terms of four metrics in Tables 1-4. Note that N/A is adopted to indicate that the method suffers from the error due to out of memory. We also compare EIML with IMVC-CBG and FIMVC-VIA

Table 5: Running time of all methods on different datasets. "N/A " denotes out of memory.

| Dataset | BSV | MIC | MKKM-IK | DAIMC | APMC | PIC | EEIMVC | $V^3$ | IMVC-CBG | FIMVC-VIA | Ours |
|---|---|---|---|---|---|---|---|---|---|---|---|
| ORL | 0.15 | 425.00 | 0.50 | 1200.00 | 0.50 | 0.30 | 0.55 | 90.00 | 3.00 | 1.70 | 0.30 |
| NGs | 0.05 | 145.00 | 0.50 | 0.20 | 0.28 | 0.25 | 0.15 | 14.50 | 1.50 | 0.30 | 0.25 |
| WebKB | 0.15 | 340.50 | 3.20 | N/A | 0.28 | 1.20 | 0.22 | 32.00 | 0.65 | 0.28 | 0.24 |
| STL10 | 66.90 | N/A | 1666.00 | 590.00 | 72.00 | 3350.00 | 68.50 | 45290.00 | 18.50 | 6.20 | 5.50 |
| MNIST | N/A | N/A | N/A | 5600.20 | N/A | N/A | N/A | N/A | 552.00 | 20.20 | 18.40 |
| Cifar100 | N/A | N/A | N/A | 25200.00 | N/A | N/A | N/A | N/A | 815.00 | 47.00 | 35.00 |

Table 6: Ablation study based on separated or unified manner

| Metrics | Manner | ORL | NGs | WebKB | STL10 | MNIST | Cifar100 |
|---|---|---|---|---|---|---|---|
| ACC | Separated manner | 70.60±0.20 | 82.45±0.30 | 82.00±0.70 | 71.40±0.55 | 84.60±0.00 | 90.40±0.45 |
| | Unified manner | 78.84±0.50 | 91.40±0.40 | 93.00±0.26 | 78.30±0.60 | 98.90±0.00 | 99.50±0.26 |
| NMI | Separated manner | 75.20±0.15 | 70.39±0.05 | 44.60±0.78 | 48.20±0.27 | 92.00±0.70 | 91.30±0.09 |
| | Unified manner | 90.15±0.60 | 77.00±0.18 | 51.20±0.50 | 59.80±0.50 | 97.30±0.10 | 99.80±0.20 |
| F1-score | Separated manner | 62.49±1.00 | 76.20±0.30 | 80.20±0.60 | 54.90±0.15 | 90.50±0.90 | 90.49±0.55 |
| | Unified manner | 71.20±0.50 | 83.20±0.70 | 90.50±0.05 | 62.50±0.50 | 99.20±0.10 | 99.60±0.20 |
| Purity | Separated manner | 70.85±0.39 | 84.20±0.64 | 82.70±0.20 | 69.40±0.90 | 88.50±0.05 | 82.40±0.19 |
| | Unified manner | 82.50±0.29 | 93.12±0.05 | 94.10±0.20 | 78.90±0.55 | 99.20±0.10 | 99.55±0.20 |

under different missing ratios on several datasets under different metrics. According to Tables 1-4 and Figs. 4-7, we draw the following conclusions:

- The proposed EIML can provide better performance than other compared methods for incomplete multi-view clustering in terms of different metrics. For instance, EIML gains a better clustering performance of 9.84% than PIC in terms of ACC on ORL, which shows that combining graph construction, anchor learning and graph partition in a unified framework of incomplete multi-view clustering is able to boost each other and result in effective clustering results.
- Compared with other methods for incomplete multi-view clustering, EIML shows better clustering performance with different missing ratios on several datasets under four metrics, which shows that the learned anchors for representing all data samples are relatively informative for these datasets and methods based on kernel or graph do not show the same satisfied performance.
- EILML produces more satisfied clustering performance than FIMVC-VIA on different datasets, showing that using the unified framework integrated by graph construction, anchor learning and graph partition can help achieving better cluster assignment matrix and this matrix can directly result in the final results.

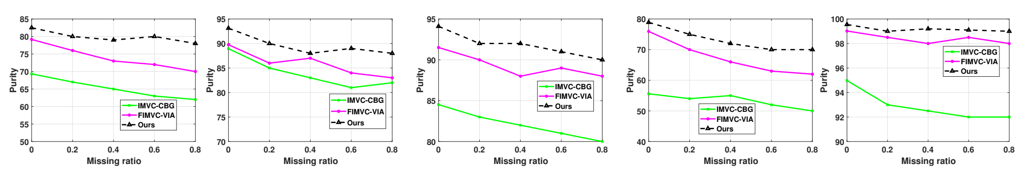


(a) ORL (b) NGs (c) WebKB (d) STL10 (e) Cifar100

Figure 7: Clustering Performance in terms of Purity on datasets with different missing ratios.

## 3.4 Running Time

In this part, we show the running time of EIML and the compared approaches on different benchmark datasets. Based on Table 5, we have the observations as follows:

- Our EIML needs less running time than other methods for incomplete multi-view clustering on different datasets in terms of ACC, which indicates its efficiency for computation cost.

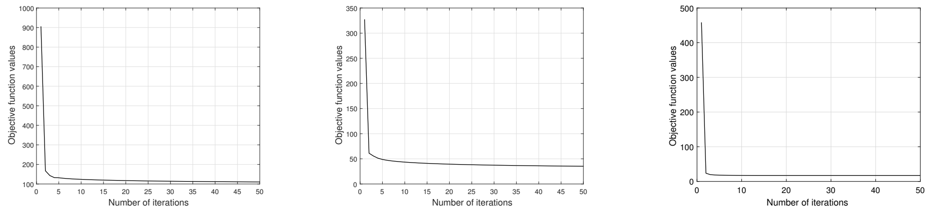


(a) ORL (b) NGs (c) WebKB

Figure 8: Convergence curve on different datasets. (a) ORL. (b) NGs. (c) WebKB.

Some other methods for comparison suffer from the memory issue on MNIST and Cifar100 based on the running time, which further shows the efficiency of our EIML.

- Some compared methods are able to consume less running time on some small dataset, i.e., EEIMVC uses less computation cost than our EIML on some datasets. However, these methods do not perform as well as ours when running on large-scale datasets. It can be explained by the fact that using a unified framework integrated by graph construction, anchor learning and graph partition can improve the efficiency for incomplete multi-view clustering, especially on the datasets with large scales .
- The dataset with larger dimensions tends to need more running time when these datasets are close in the size, i.e, IMVC-CBG needs more running time on Cifar100 than MNIST and the latter dataset has smaller dimension than the former dataset. As the size of dataset increases, our EIML and the compared methods usually consume more running time on different datasets.

### 3.5 Ablation Study

In this section, we perform ablation study to validate the superiority of adopting a unified framework integrated by graph construction, anchor learning and graph partition. In comparative experiments, we first learn anchors and construct the graph to obtain informative representation. Then the graph partition is isolated from the above two processes in the designed experiment. According to Table 6, we can find that the clustering performance of the proposed EIML significantly outperforms than the case in separated manner, demonstrating the necessarity of using a unified framework integrated by graph construction, anchor learning and graph partition to directly achieve the final assignment.

### 3.6 Convergence Analysis

We conduct convergence analysis of EIML on different datasets by showing the evolution process of the objective function with iterations in terms of ACC. According to Fig. 8, we observe that EIML monotonically decreases with iterations and tends to converge in about some iterations on these datasets, which demonstrates the convergence of EIML.

## 4 Conclusion

we propose EIML in this work for efficient incomplete multi-view clustering. It simultaneously considers graph construction, anchor learning and graph partition in a unified framework, in which these parts boost each other for improving the effectiveness and efficiency for datasets with large scales. To be specific, a shared anchor graph for guaranteeing the consistency among multiple views is learned and the adaptive weight coefficient is adopted to balance the impact for each view. We then adopt the alternative algorithm to solve the optimization problem. Extensive experiments on several benchmark datasets show the effectiveness and efficiency of EIML under different metrics.

## REFERENCES

Yongyong Chen, Xiaolin Xiao, and Yicong Zhou. Multi-view subspace clustering via simultaneously learning the representation tensor and affinity matrix. *Pattern Recognit.*, 106:107441, 2020.

Yongyong Chen, Xiaolin Xiao, Chong Peng, Guangming Lu, and Yicong Zhou. Low-rank tensor graph learning for multi-view subspace clustering. *IEEE Transactions on Circuits and Systems for Video Technology*, 32(1):92–104, 2022.

Xiang Fang, Yuchong Hu, Pan Zhou, and Dapeng Oliver Wu. V$ˆ3$h: View variation and view heredity for incomplete multiview clustering. *IEEE Trans. Artif. Intell.*, 1(3):233–247, 2020.

Jun Guo and Jiahui Ye. Anchors bring ease: An embarrassingly simple approach to partial multi-view clustering. In *The AAAI Conference on Artificial Intelligence*, pp. 118–125, 2019.

Menglei Hu and Songcan Chen. Doubly aligned incomplete multi-view clustering. In *Proceedings of the International Joint Conference on Artificial Intelligence*, pp. 2262–2268, 2018.

Yuheng Jia, Guanxing Lu, Hui Liu, and Junhui Hou. Semi-supervised subspace clustering via tensor low-rank representation. *IEEE Transactions on Circuits and Systems for Video Technology*, 33 (7):3455–3461, 2023.

Zhao Kang, Wangtao Zhou, Zhitong Zhao, Junming Shao, Meng Han, and Zenglin Xu. Large-scale multi-view subspace clustering in linear time. In *The AAAI Conference on Artificial Intelligence*, pp. 4412–4419, 2020.

Abhishek Kumar, Piyush Rai, and Hal Daumé III. Co-regularized multi-view spectral clustering. In *Advances in Neural Information Processing Systems*, pp. 1413–1421, 2011.

Miaomiao Li, Siwei Wang, Xinwang Liu, and Suyuan Liu. Parameter-free and scalable incomplete multiview clustering with prototype graph. *IEEE Transactions on Neural Networks and Learning Systems*, pp. 1–11, 2022.

Shao-Yuan Li, Yuan Jiang, and Zhi-Hua Zhou. Partial multi-view clustering. In *Proceedings of the AAAI Conference on Artificial Intelligence*, pp. 1968–1974, 2014.

Yijie Lin, Yuanbiao Gou, Zitao Liu, Boyun Li, Jiancheng Lv, and Xi Peng. COMPLETER: incomplete multi-view clustering via contrastive prediction. In *IEEE Conference on Computer Vision and Pattern Recognition*, pp. 11174–11183, 2021.

Suyuan Liu, Xinwang Liu, Siwei Wang, Xin Niu, and En Zhu. Fast incomplete multi-view clustering with view-independent anchors. *IEEE Transactions on Neural Networks and Learning Systems*, pp. 1–12, 2022.

Xinwang Liu, Miaomiao Li, Lei Wang, Yong Dou, Jianping Yin, and En Zhu. Multiple kernel k-means with incomplete kernels. In *Proceedings of the AAAI Conference on Artificial Intelligence*, pp. 2259–2265, 2017.

Xinwang Liu, Miaomiao Li, Chang Tang, Jingyuan Xia, Jian Xiong, Li Liu, Marius Kloft, and En Zhu. Efficient and effective regularized incomplete multi-view clustering. *IEEE Trans. Pattern Anal. Mach. Intell.*, 43(8):2634–2646, 2021.

Shirui Luo, Changqing Zhang, Wei Zhang, and Xiaochun Cao. Consistent and specific multi-view subspace clustering. In *Proceedings of the AAAI Conference on Artificial Intelligence*, pp. 3730–3737, 2018.

Ziyu Lv, Quanxue Gao, Xiangdong Zhang, Qin Li, and Ming Yang. View-consistency learning for incomplete multiview clustering. *IEEE Transactions on Image Processing*, 31:4790–4802, 2022. doi: 10.1109/TIP.2022.3187562.

Zhengrui Ma, Zhao Kang, Guangchun Luo, and Ling Tian. Towards clustering-friendly representations: Subspace clustering via graph filtering. *CoRR*, abs/2106.09874, 2021.

Andrew Y. Ng, Michael I. Jordan, and Yair Weiss. On spectral clustering: Analysis and an algorithm. In *Advances in Neural Information Processing Systems*, pp. 849–856, 2001.

Feiping Nie, Guohao Cai, and Xuelong Li. Multi-view clustering and semi-supervised classification with adaptive neighbours. In *Proceedings of the AAAI Conference on Artificial Intelligence*, pp. 2408–2414, 2017.

Feiping Nie, Shaojun Shi, and Xuelong Li. Auto-weighted multi-view co-clustering via fast matrix factorization. *Pattern Recognit.*, 102:107207, 2020.

Yalan Qin, Hanzhou Wu, Xinpeng Zhang, and Guorui Feng. Semi-supervised structured subspace learning for multi-view clustering. *IEEE Trans. Image Process.*, 31:1–14, 2022.

Yalan Qin, Chuan Qin, Xinpeng Zhang, Donglian Qi, and Guorui Feng. Nim-nets: Noise-aware incomplete multi-view learning networks. *IEEE Trans. Image Process.*, 32:175–189, 2023.

Weixiang Shao, Lifang He, and Philip S. Yu. Multiple incomplete views clustering via weighted nonnegative matrix factorization with $l_2$, 1 regularization. In *Machine Learning and Knowledge Discovery in Databases - European Conference, ECML PKDD*, volume 9284, pp. 318–334. Springer, 2015.

Mengjing Sun, Pei Zhang, Siwei Wang, Sihang Zhou, Wenxuan Tu, Xinwang Liu, En Zhu, and Changjian Wang. Scalable multi-view subspace clustering with unified anchors. In *ACM Multimedia Conference*, pp. 3528–3536, 2021.

Hao Wang, Linlin Zong, Bing Liu, Yan Yang, and Wei Zhou. Spectral perturbation meets incomplete multi-view data. In *Proceedings of the International Joint Conference on Artificial Intelligence*, pp. 3677–3683, 2019.

Hua Wang, Feiping Nie, Heng Huang, and Fillia Makedon. Fast nonnegative matrix tri-factorization for large-scale data co-clustering. In *Proceedings of the International Joint Conference on Artificial Intelligence*, pp. 1553–1558, 2011.

Shuqin Wang, Yongyong Chen, Zhiping Lin, Yigang Cen, and Qi Cao. Robustness meets low-rankness: Unified entropy and tensor learning for multi-view subspace clustering. *IEEE Transactions on Circuits and Systems for Video Technology*, 33(11):6302–6316, 2023.

Siwei Wang, Xinwang Liu, Li Liu, Wenxuan Tu, Xinzhong Zhu, Jiyuan Liu, Sihang Zhou, and En Zhu. Highly-efficient incomplete largescale multiview clustering with consensus bipartite graph. In *2022 IEEE/CVF Conference on Computer Vision and Pattern Recognition (CVPR)*, pp. 9766–9775, 2022a.

Siwei Wang, Xinwang Liu, Xinzhong Zhu, Pei Zhang, Yi Zhang, Feng Gao, and En Zhu. Fast parameter-free multi-view subspace clustering with consensus anchor guidance. *IEEE Trans. Image Process.*, 31:556–568, 2022b.

Cai Xu, Ziyu Guan, Wei Zhao, Hongchang Wu, Yunfei Niu, and Beilei Ling. Adversarial incomplete multi-view clustering. In *Proceedings of the International Joint Conference on Artificial Intelligence*, pp. 3933–3939, 2019.

Jie Xu, Chao Li, Liang Peng, Yazhou Ren, Xiaoshuang Shi, Heng Tao Shen, and Xiaofeng Zhu. Adaptive feature projection with distribution alignment for deep incomplete multi-view clustering. *IEEE Transactions on Image Processing*, 32:1354–1366, 2023.

Yongkai Ye, Xinwang Liu, Jianping Yin, and En Zhu. Co-regularized kernel k-means for multi-view clustering. In *International Conference on Pattern Recognition*, pp. 1583–1588, 2016.

Shengju Yu, Siwei Wang, Yi Wen, Ziming Wang, Zhigang Luo, En Zhu, and Xinwang Liu. How to construct corresponding anchors for incomplete multiview clustering. *IEEE Transactions on Circuits and Systems for Video Technology*, pp. 1–1, 2023.

Chen Zhang, Siwei Wang, Jiyuan Liu, Sihang Zhou, Pei Zhang, Xinwang Liu, En Zhu, and Changwang Zhang. Multi-view clustering via deep matrix factorization and partition alignment. In *ACM Multimedia Conference*, pp. 4156–4164, 2021a.

Pei Zhang, Siwei Wang, Jingtao Hu, Zhen Cheng, Xifeng Guo, En Zhu, and Zhiping Cai. Adaptive weighted graph fusion incomplete multi-view subspace clustering. *Sensors*, 20(20):5755, 2020.

Yi Zhang, Xinwang Liu, Siwei Wang, Jiyuan Liu, Sisi Dai, and En Zhu. One-stage incomplete multi-view clustering via late fusion. In *ACM Multimedia Conference*, pp. 2717–2725, 2021b.

Handong Zhao, Zhengming Ding, and Yun Fu. Multi-view clustering via deep matrix factorization. In *Proceedings of the AAAI Conference on Artificial Intelligence*, pp. 2921–2927, 2017.

Xiaojia Zhao, Qiangqiang Shen, Yongyong Chen, Yongsheng Liang, Junxin Chen, and Yicong Zhou. Self-completed bipartite graph learning for fast incomplete multi-view clustering. *IEEE Transactions on Circuits and Systems for Video Technology*, pp. 1–1, 2023.

Sihang Zhou, Xinwang Liu, Miaomiao Li, En Zhu, Li Liu, Changwang Zhang, and Jianping Yin. Multiple kernel clustering with neighbor-kernel subspace segmentation. *IEEE Trans. Neural Networks Learn. Syst.*, 31(4):1351–1362, 2020.